

Small accessible urban parks mitigate heat-related mortality

Received: 15 April 2025

Accepted: 1 December 2025

Published online: 15 January 2026

 Check for updates

Cheng He^{1,2,7}, Peng Yin^{3,7}, Renjie Chen^{1,7}, Li Wang⁴, Yuan Wang⁵, Alexandra Schneider^{1,2}, Haidong Kan^{1,6}✉ & Maigeng Zhou^{1,3}✉

Increasing evidence suggests that a city's green space coverage can effectively regulate heatwave-related health risk, but the spatial pattern of green spaces has not received sufficient attention. Here we investigated how different green space configurations modify heatwave-related mortality risk across 265 Chinese cities using five landscape metrics. We evaluated heatwaves using varying intensities and durations. Results showed that cities with higher green space coverage (percentage of landscape, PLAND), more dispersed distributions (higher splitting index, SPLIT) and more regular boundaries (lower landscape shape index, LSI) showed significantly lower heatwave-related mortality risks. For heatwaves with ≥ 92.5 th percentile temperature for ≥ 2 consecutive days, mortality risks were substantially higher in cities with low PLAND (relative risk (RR) 1.11, 95% confidence interval (CI) 1.08–1.14), low SPLIT (RR 1.10, 95% CI 1.08–1.13) and high LSI (RR 1.13, 95% CI 1.10–1.18) compared with their counterparts with high PLAND (RR 1.04, 95% CI 1.01–1.07), high SPLIT (RR 1.04, 95% CI 1.01–1.08) and low LSI (RR 1.04, 95% CI 0.96–1.12), respectively; all $P < 0.05$. Notably, merely increasing green space quantity (patch density) or largest patch size (largest patch index) did not significantly reduce mortality risk. Our findings emphasize that green space configuration, beyond total coverage, plays a crucial role in mitigating heatwave-related mortality, suggesting that urban planning should prioritize strategically distributed, more dispersed green spaces with regular boundaries rather than simply focusing on quantity and the size of the largest green patches to enhance public health resilience against increasing heatwave threats.

As global climate change intensifies, heatwave events are becoming more frequent¹, posing a serious threat to human health². Moreover, the global urbanization process is leading to excessive anthropogenic heat emissions and an increase in impervious surfaces, exacerbating the urban heat island effect^{3,4} and consequently elevating the risks of heat-related illnesses and mortality⁵, especially among the elderly and those with pre-existing conditions^{6,7}. In this context, green spaces, serving as an effective natural regulatory mechanism⁸, are increasingly recognized for their potential to mitigate heat exposures⁹, improve the

quality of the living environment quality and reduce heatwave-related mortality risks^{10,11}.

The pathways through which green space mitigates health risks associated with high temperatures manifest in several ways. First, the transpiration from concentrated vegetation can directly cool the surrounding area, thus minimizing the effects of nearby heat exposure directly¹². In addition, green spaces offer cool refuges, which can alleviate the residents' mental stress during heatwaves and provide venues for necessary information dissemination and community interaction,

A full list of affiliations appears at the end of the paper. ✉e-mail: kanh@fudan.edu.cn; zhoumaigeng@ncncc.chinacdc.cn

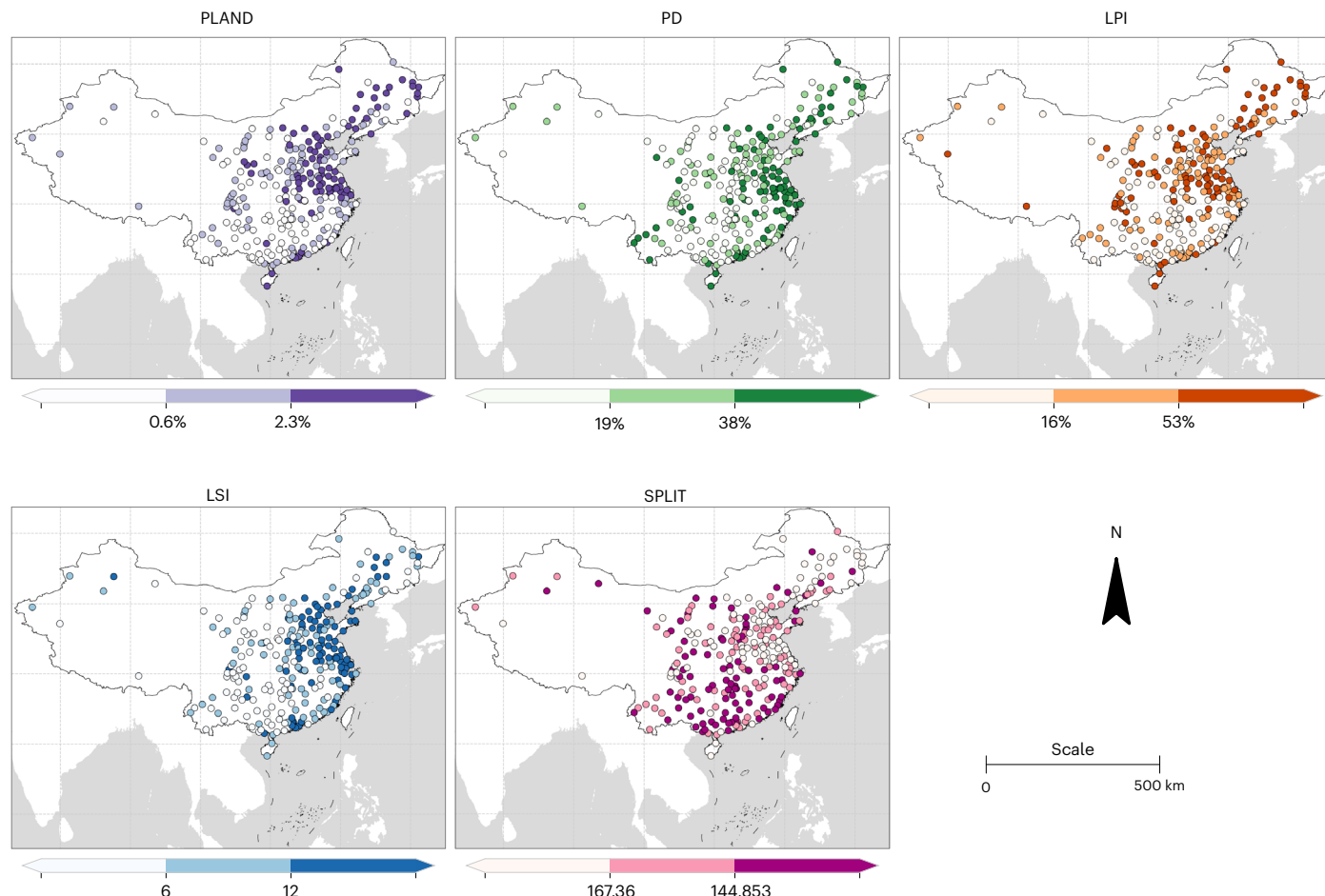


Fig. 1 | Values of 5 landscape metrics for green space in 265 cities. The selection of the five landscape metrics prioritized key factors: overall green coverage, patch quantity, predominant patch features, shape complexity or fragmentation,

and spatial continuity. Calculation methods for each landscape metric are detailed in Methods. All landscape metrics are divided into three equal groups: low, medium and high, based on tertile distribution.

increasing the likelihood that residents help each other during disasters and potentially enhancing overall resilience to heat^{13,14}. Previous studies have indicated that the cooling benefits of green spaces are not uniformly distributed¹⁵. Their impact is contingent upon the layout and scale, such as the concentration, shape and density of green patches, all of which may influence the local cooling effect¹⁵. Therefore, it is logical to hypothesize that different green space layouts may have varying influences on heatwave-related health risks. Current studies primarily focus on the role of green space landscape patterns in regulating overall surface temperature or the thermal environment¹⁶. However, as mentioned, green spaces regulate the health impacts of high temperatures not only through direct cooling but also by providing refuges and alleviating mental stress for residents. This may require landscape patterns that go beyond simply maximizing the average cooling effect. In other words, the pattern most effective at providing overall cooling may not necessarily be the best at mitigating heat-related health impacts across the city.

While existing epidemiological evidence supports the health benefits of green spaces, research has often focused primarily on overall greenness coverage¹⁷. Recent studies have begun to explore the relationship between various aspects of green space morphology and health outcomes¹⁸. For instance, connectivity, aggregation, coherence and shape complexity of green spaces have been associated with non-communicable diseases¹⁹. Greater distances between shrublands have been linked to more frequent mental distress²⁰, and more fragmented green space morphology has been associated with shorter life expectancy²¹. In addition, the morphology of green spaces has been found

to influence mortality rates of cardiovascular diseases, which may be mediated by the combined effects of air pollution and temperature²². Despite these findings, there is currently a lack of research examining the relationship between green space patterns and heatwave-related health outcomes. Because heatwaves are an increasingly notable public health challenge and green spaces offer effective cooling, addressing this knowledge gap could provide crucial insights for future green space planning and climate adaptation measures.

Therefore, this study is among the first to comprehensively examine the relationship between green space layouts and heatwave-related mortality risks across multiple cities. By integrating landscape ecology and epidemiological approaches, we aimed to thoroughly analyse the potential impacts of various green space metrics on the mortality risk related to heatwaves with different intensities and durations. This study seeks to provide valuable insights for green space planners and policymakers, potentially informing strategies to enhance green space configurations and improve resilience against the adverse health impacts of heatwave events. The results could help improve adaptation to climate warming through urban planning.

Results

Descriptive statistics

Our study utilized mortality data from China's Death Surveillance Points System (2013–2019) across 265 major Chinese cities. We assessed green space distribution using a parcel-level land use classification dataset with 10-m resolution. To capture critical aspects of green space configuration, we screened potential landscape metrics based on their

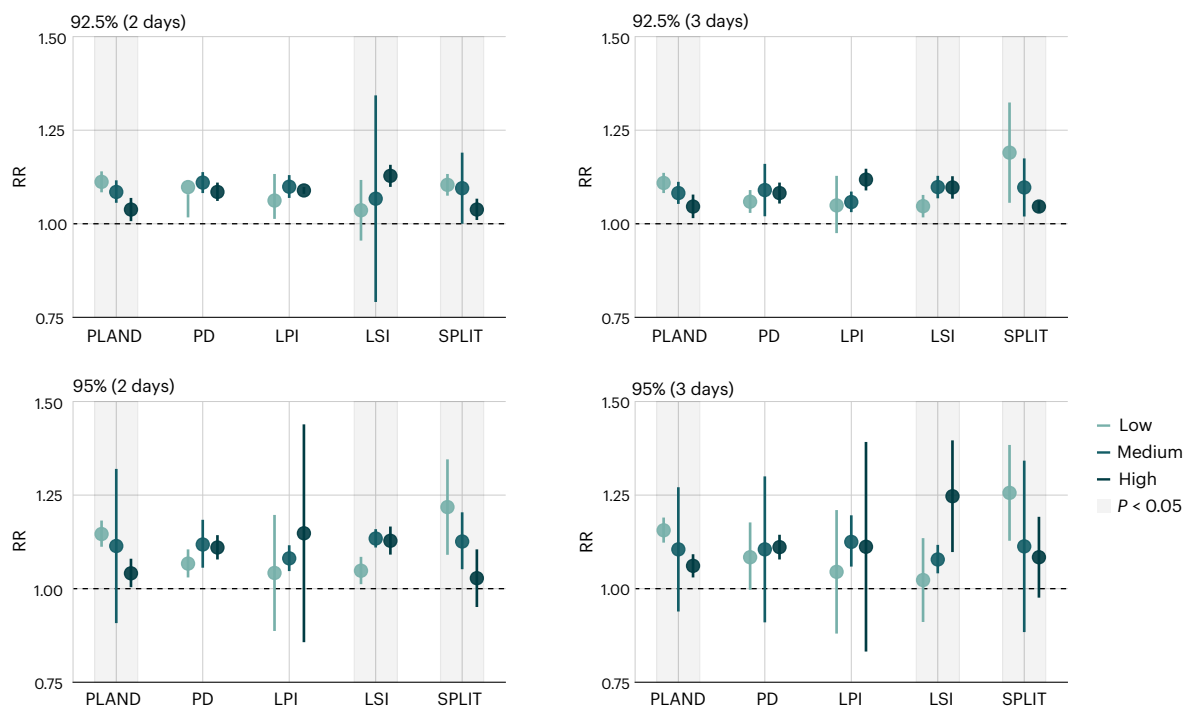


Fig. 2 | Overall cumulative heatwave-mortality relationship by different green space metrics. All cities were grouped based on the evaluation results of five landscape metrics for green space distribution. Data are presented as RRs (centre points) with 95% CIs (vertical lines). Meta-regression analysis provided results for each group, with a grey background indicating significant differences in heatwave risk ($P < 0.05$, two-sided multivariate Wald tests). The analysis

incorporated heatwave definition with two thresholds (92.5% and 95%) and two durations (2 days and 3 days). The landscape metrics included PLAND, PD, LPI, LSI and SPLIT. All landscape metrics are divided into three equal groups: low, medium and high, based on tertile distribution. Detailed numerical values and P values for all comparisons are provided in Supplementary Table 7.

ability to represent four key attributes: size, shape, aggregation and fragmentation. This process led us to select five complementary metrics: percentage of landscape (PLAND), measuring overall coverage; patch density (PD), reflecting patch quantity; largest patch index (LPI), indicating dominance of the largest patch; landscape shape index (LSI), assessing boundary complexity; and splitting index (SPLIT), measuring spatial fragmentation. The calculation methods for each landscape metric are detailed in Methods, and their spatial implications are illustrated in Extended Data Fig. 1. We used a two-stage analytical framework: first examining city-specific associations between heatwaves and mortality, and then pooling these estimates through meta-regression to explore how different green space landscape metrics modified heatwave-related mortality risks. For detailed explanations of our metrics selection and methodological approaches, please refer to Methods.

Among all these included sites, 2 of the included cities are in the tropical region, 145 in the temperate climatic zone, 91 in the continental climatic zone and 27 in the arid zones (Supplementary Fig. 1). The green space landscape metrics across these cities are illustrated in Fig. 1. There are considerable variations, for PLAND that ranges from 0.02% to 38.15%, for PD that ranges from 0.02 to 1.76, for LPI that ranges from 1.01% to 11.37% and for LSI that ranges from 1.43 to 77.02. Moreover, the SPLIT index varied more significantly, from 60,65 to 58,420,387. The correlation matrix heatmap of five selected landscape metrics (Supplementary Fig. 2) suggested no significant collinearity among the metrics after they were categorized into three probability-based levels, considering that all correlation coefficients were less than 0.65. The variance inflation factor (VIF) analysis further confirmed low multicollinearity, with all VIF values below 1.5 (PLAND 1.405, PD 1.253, LPI 1.169, LSI 1.297, SPLIT 1.003), well below the commonly accepted threshold of 5 (Supplementary Table 1).

Overall heatwave-mortality associations

Our analysis incorporated data on 11,917,035 non-accidental daily deaths, with 2,914,435 deaths among individuals aged 5–65 years and

9,002,600 deaths in those aged over 65. As shown in Table 1 and Supplementary Fig. 3, the spatial distribution of two thresholds for heatwave definitions exhibits a similar pattern, with higher thresholds in southern than northern regions and higher thresholds in coastal areas than inland regions. Our analysis demonstrated that all four definitions of heatwave events, including two percentiles (95% and 97.5%) and two different durations (2 days and 3 days), significantly increased daily mortality rates, with the relative risk (RR) ranging from 1.12 (95% confidence interval (CI) 1.08–1.17) for a heatwave event with 95% percentile and 2-day duration to 1.20 (95% CI 1.16–1.24) for 97.5% percentile and 3-day duration event. In addition, heatwave events defined by the 97.5% percentile had higher RR compared with those of 95% percentile, and longer-duration heatwaves (3 days) had greater impacts on daily mortality than shorter-duration heatwaves (2-day). Moreover, greater risks were observed in older adults (Supplementary Table 2).

Green space configuration and heatwave-related mortality

As depicted in Fig. 2, the associations between green space landscape patterns and heatwave-related mortality risks exhibit similar trends across heatwaves of different intensities and durations. For all four heatwave definitions, we consistently observed that cities with higher PLAND experienced significantly lower heatwave-related mortality risk compared with those with lower PLAND ($P < 0.05$). In addition, cities with higher values of LSI showed significantly higher mortality risks than those with lower LSI across most heatwave definitions. Moreover, for the SPLIT classifications, cities with lower SPLIT demonstrated significantly higher risks than those with higher values in several heatwave scenarios. Notably, no significant differences between groups were observed under any of the four heatwave definitions when cities were categorized according to PD and LPI.

As depicted in Fig. 3, the direction of the between-group differences is consistent across both age groups, with between-group differences being more pronounced in the older age group. Among

Table 1 | Descriptive statistics of heatwave case days in cities under four different definitions

	92.5% (2 days)	92.5% (3 days)	95% (2 days)	95% (3 days)
PLAND				
Low (<0.6%)	15,360 (88)	12,916 (88)	9,824 (88)	7,886 (88)
Medium (0.6%–2.3%)	15,392 (89)	13,092 (89)	9,996 (89)	8,102 (89)
High (>2.3%)	15,440 (88)	13,390 (88)	9,932 (88)	8,112 (88)
PD				
Low (<19%)	15,276 (88)	12,898 (88)	9,792 (88)	7,852 (88)
Medium (19%–38%)	15,429 (89)	13,109 (89)	9,969 (89)	7,991 (89)
High (>38%)	15,487 (88)	13,391 (88)	9,991 (88)	8,257 (88)
LPI				
Low (<16%)	15,303 (88)	12,869 (88)	9,814 (88)	7,896 (88)
Medium (16%–53%)	15,479 (89)	13,237 (89)	10,026 (89)	8,122 (89)
High (>53%)	15,410 (88)	13,292 (88)	9,912 (88)	8,082 (88)
LSI				
Low (<6)	15,210 (88)	12,808 (88)	9,785 (88)	7,825 (88)
Medium (6–12)	15,576 (89)	13,252 (89)	9,887 (89)	7,983 (89)
High (>12)	15,406 (88)	13,338 (88)	10,080 (88)	8,292 (88)
SPLIT				
Low (<16,736)	15,431 (88)	13,349 (88)	9,918 (88)	8,080 (88)
Medium (16,736–144,853)	15,443 (89)	13,231 (89)	10,073 (89)	8,249 (89)
High (>144,853)	15,318 (88)	12,818 (88)	9,761 (88)	7,771 (88)

Shown is the total number of heatwave days identified during the study period. All landscape metrics are divided into three equal groups: low, medium and high, based on tertile distribution.

the three main climate zones, the trends of heatwave-related mortality risks align with the overall findings, primarily in risk differences observed for classifications of PLAND, LSI and LPI. However, some of these between-group differences did not reach statistical significance, probably due to the number of cities available. In addition, sensitivity analyses demonstrated the robustness of our findings. Using daily maximum temperature instead of daily mean temperature to define heatwaves, or employing population-weighted meteorological data within city boundaries, did not significantly alter our results (Supplementary Table 3). Furthermore, adjusting key statistical model parameters—such as modifying the degrees of freedom for the lag-response function and extending the lag period to 14 days—did not alter our main conclusions (Supplementary Table 4). Moreover, controlling for daily PM_{2.5} (particulate matter $\leq 2.5 \mu\text{m}$ in aerodynamic diameter) concentrations and using a different green space dataset (Global Forest Change dataset) yielded consistent results (Supplementary Table 5), further validating our findings, despite differences in some metric calculations between the two datasets (Supplementary Table 6).

Discussion

Our analysis in 265 Chinese cities reveals a significant link between landscape patterns for green space and mortality risks associated with heatwaves of varying thresholds and durations. The results indicate that heatwave-related mortality risk may be influenced not only by overall green space coverage but also by the average shape and clustering of green spaces. Specifically, cities with higher green space coverage, more dispersed layouts and more regular boundaries showed lower heatwave-related mortality risks. However, increasing the number

of green spaces or enlarging the largest patch does not significantly impact overall heatwave-related mortality risk. These findings contribute to existing knowledge on the health benefits of green space amid extreme heat events, underscoring the critical role of optimizing green space configurations to reduce heatwave mortality risks.

Our findings are consistent with previous studies suggesting that green spaces could significantly improve health outcomes. Increased accessibility to green areas has been shown to mitigate the risk of various diseases, including cardiovascular^{23,24} and respiratory diseases²⁵. Furthermore, there is substantial evidence indicating that increasing greenery coverage can effectively reduce heat-related mortality. For instance, recent research demonstrated that a 10% increase in tree canopy coverage significantly reduced heat-related mortality in North America, particularly in densely populated urban areas²⁶. A study in Lisbon, Portugal, found that green space significantly alleviated heat-related mortality among the elderly population over 65 years²⁷. A study encompassing 452 locations worldwide indicated that a 20% augmentation of green space was linked to a 9.02% (95% CI 8.88–9.16) reduction in the mortality fraction attributable to ambient heat¹⁷. All these findings consistently support that increased greenery coverage could notably diminish health risks associated with heatwaves. However, most previous epidemiological studies have primarily focused on overall greenness coverage rather than the spatial configuration of green spaces, which could provide more actionable insights for adaptive measures and future green space planning. Moreover, our findings diverge from previous studies that focus on the cooling efficiency of green spaces¹⁵, which emphasize the importance of larger green patches and lower SPLIT values in significant average cooling across cities^{15,28}. Contrary to these studies, our research did not observe a substantial moderating effect of the LPI on heat-related mortality risks. Interestingly, we found that a higher SPLIT value could more effectively alleviate health impacts. This suggests that the health benefits of green spaces extend beyond mere temperature regulation, highlighting the complexity of how green space configuration influences health outcomes.

Several plausible explanations help us understand how different metrics of green spaces could influence their roles in modifying the health impacts of heatwaves. First, an increase in the PLAND value indicates greater green coverage, which enhances the capacity for transpiration, effectively moderating temperature rises during heatwave periods²⁹. It may also imply greater average accessibility to green space³⁰, thereby effectively reducing the average heat exposure health risk for city dwellers. Second, an increase in the SPLIT metric indicates that green spaces are more scattered, which can expand average accessibility to greenery across a broader region³¹. This widespread distribution of green spaces is potentially beneficial, especially during heatwaves, as it could provide necessary shade and cooling to a larger portion of the population. Accessible dispersed green spaces, or cooling centres, can be particularly vital for those who must engage in outdoor activities during extreme heat days, by virtue of offering respite and reducing the risk of heat exposure³². Moreover, dispersed green spaces can serve as relaxation spots that help mitigate the psychological and physiological stresses induced by high temperatures³³. This contrasts with the impact of concentrated green spaces, which, despite their ability to significantly lower overall average temperatures, may not be as effective in enhancing overall livability as increased accessibility to multiple green areas. This point could be further corroborated by our findings regarding the LPI, which did not reveal a significant moderating effect, but suggested that the distribution of green spaces is more crucial for health benefits during heat events than the presence of singular large green areas. Third, a higher LSI suggested more regular and intact boundaries of green spaces, enhancing vegetation's transpiration process. When these boundaries are fragmented, the cooling effects can be diminished by the surrounding environment^{34,35}, reducing their average ability to provide relief during heatwave days. Moreover, the effectiveness of green spaces in

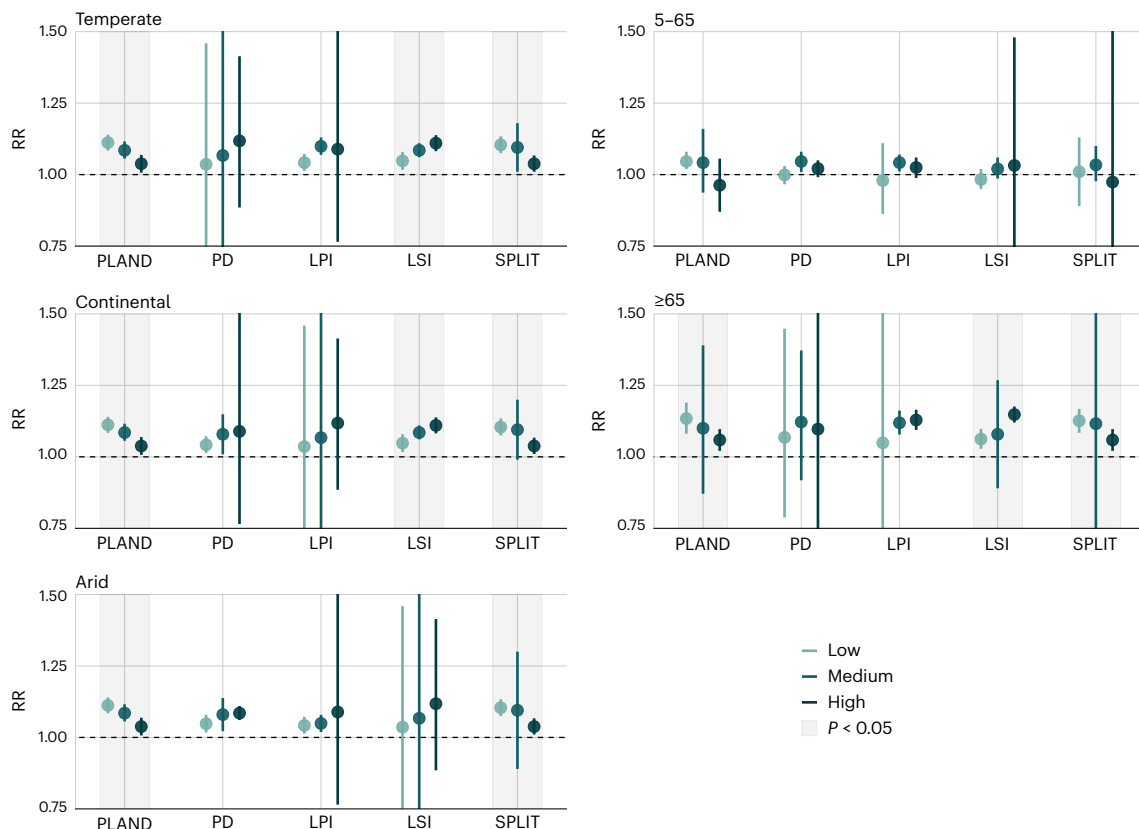


Fig. 3 | Overall cumulative heatwave-mortality relationship by different green space metrics across different climate zones and age groups. Subgroup analysis under the definition of heatwaves with thresholds of 92.5% percentile of daily mean temperature and duration of three days. Data are presented as RRs (centre

points) with 95% CIs (vertical lines). Climate zoning is primarily based on the Köppen climate classification. Grey background indicates significant differences in heatwave risk ($P < 0.05$). The landscape metrics include PLAND, PD, LPI, LSI and SPLIT. Detailed numerical values are provided in Supplementary Tables 8 and 9.

mitigating high temperatures and providing shade depends on their size and continuity³⁶. Thus, increasing PD without considering their overall configuration could not substantially mitigate the adverse health effects of high temperatures.

Anthropogenic climate change significantly increases the frequency, duration and intensity of heatwaves globally, and thus the heat-related disease burden would markedly increase, especially when considering the growing urban heat island effects due to worldwide urbanization³⁷. Therefore, understanding the effectiveness of green space planning in influencing the health risks associated with heatwaves is crucial for better addressing climate warming. Our findings have substantial implications for future land use planning policies. First, our results highlight that increasing overall green coverage can effectively reduce the health impacts of various heatwaves, regardless of their duration or thresholds. Thus, strategically increasing average greenery remains a vital method for mitigating future warming-related health risks. Second, the effectiveness of green space relies more on their thoughtful design than on mere quantity. Proper planning should emphasize the creation of accessible, community-based cooling refuges that not only contribute to revitalizing health services but also support mutual assistance and information exchange within communities during extreme heat events. It is important to avoid fragmented and irregularly distributed green spaces, as they often fail to provide these comprehensive benefits. Lastly, our research suggests that, although a more dispersed layout of green spaces can alleviate overall health risks, merely enlarging the area of a single large park may not effectively address these risks. Therefore, future planning should aim to enhance the average accessibility of green spaces for all residents, focusing on improving the configuration of multiple smaller parks rather than solely expanding large parks. Overall, community-based

dispersed cooling centres are more beneficial than centralized, large green spaces.

This study has several limitations that should be noted. First, while it included a substantial number of cities and explored potential differences across several different climatic zones, the influence of various climate conditions on the observed trends was not identified. More cities need to be included in future research to examine potential variations in vegetation transpiration mechanisms across different climates. Second, all the cities in this study are located in mainland China; therefore, the results may not be easily generalizable to other regions with different climatic conditions, lifestyles and healthcare resources. Third, the impact of green spaces on heatwaves may change as urbanization progresses, and our data, limited to recent impacts, might not fully capture these dynamics.

In conclusion, this nationwide study in China underscores the importance of green spaces in reducing heatwave-related mortality risks. We found that both the overall coverage of green spaces and their spatial configuration and layout are associated with heat-related health impacts. Cities with higher green space coverage, dispersed green space layouts and more regular boundaries demonstrated lower mortality risks during heatwaves. Conversely, simply increasing the number of green spaces or enlarging a single large park may not significantly alleviate heatwave-related mortality risks. Our findings challenge conventional notions that focus solely on green space coverage in health promotion and suggest a more nuanced perspective that the distribution and configuration of greenery should be considered in the health risk assessment of heatwaves and the planning of greenness. This indicates that future urban planning should prioritize strategically dispersed green spaces that enhance accessibility, thereby providing broader cooling effects. These insights contribute to our

understanding of urban health amid climate change, emphasizing the need for adaptable, resilient land use planning to combat the health threats due to the increasing frequency and severity of heatwaves.

Methods

Health outcome data

This study utilized daily mortality data from a national death registry, the Death Surveillance Points System, from 2013 to 2019, which covers all cities in mainland China at the prefecture level or above³⁸. To ensure its adequate representation at different levels, the Disease Surveillance Points System included districts and counties from almost all cities at or above the prefecture level³⁹. All these surveillance points were selected by an iterative method involving multistage stratification that took into account the sociodemographic characteristics of the total population in each city³⁹. This well-established death registry dataset have been widely used in policy formulation and disease burden assessment related to different environmental exposures in China^{40–43} and worldwide⁴⁴. Specifically, daily death records due to non-accidental causes, categorized under codes A00–R99 according to the International Classification of Diseases-10, were extracted for analysis. We also divided daily total deaths into strata by age ranges (5–64 years, 65 years or older). Deaths among children under age 5 were too few and were therefore excluded from our analysis. For this study, we utilized a well-established mortality dataset encompassing 265 cities from this dataset⁴¹. To ensure enough statistical power when fitting time-series study design, we excluded cities with fewer than 3 total deaths on average per day and with a total population of at least 200,000 (ref. 40) and 7 cities with insufficient green space areas (total coverage <0.01%). In summary, these cities are dispersed across all 31 provincial administrative regions and account for >80% of all cities at the prefecture level and above in China. The average population of these 265 cities during the study period was 3,413,322, with a range from 509,639 to 29,454,867.

Green space and its morphology

We obtained data on the spatial distribution of green spaces in each city from the Essential Urban Land Use Categories in China (EULUC-China) dataset, a widely used parcel-level land use classification dataset in China⁴⁵. This dataset was developed by the Future Urbanity & Sustainable Environment Group using 10-m satellite images, OpenStreetMap, nighttime light images, points of interest and Tencent mobile-phone location request data. Several methods were used, including parcel generation using the OpenStreetMap road network and impervious boundaries, as well as crowdsourced collection of training data⁴⁵. It categorizes land use into 5 main and 12 second-level types with a 10-m resolution for 2018. Due to the detailed information, it has been utilized in numerous studies to represent the period of 2010s⁴⁶ across different themes^{46–48}. For our research, we specifically used the 'Park and green space' category from the second-level classification as the basis for our green space spatial data. This category primarily represents parks and green space lands used for entertainment and environmental conservation. It includes all large green parks and urban green parcels identified by combining polygon-based parcels from the OpenStreetMap road network with remote sensing data. This classification specifically excludes urban waterbodies and blue spaces, allowing us to focus on the effects of green space without confounding from water features⁴⁶. Due to the spatial resolution limitations of the data (10 m), smaller-scale neighbourhood parcels and street trees are not included in this dataset.

We chose this dataset over traditional remote-sensing-based land use data for our primary analysis because the EULUC-China dataset captures green space distribution not only based on physical characteristics from remote sensing images but also on actual usage patterns from visitor records. Consequently, it provides a more reliable foundation for our study on the relationship between green space layout and heatwave-related mortality risks, as it closely aligns with real-world land use patterns.

A relevant review indicates that studies on the health effects of green space typically consider landscape metrics from six aspects: size, shape, aggregation, connectedness, diversity and fragmentation¹⁸. Based on their effectiveness observed in epidemiological studies and our specific research needs on undifferentiated green spaces, we focused on four of these aspects: size, shape, aggregation and fragmentation. We chose the specific metrics due to the prior knowledge^{20,21,49,50} and the potential non-collinearity among the metrics. As a result, we selected the following five metrics:

(1) PLAND

$$\text{PLAND} = \frac{\sum_{i=1}^n A_i}{A_{\text{total}}} \times 100\%$$

A_i is the area of the i th patch of the green space, A_{total} is the total landscape area and n is the total number of green space patches within the city boundaries. This index is calculated as a percentage, reflecting the proportion of the total city landscape constituted by green spaces. It is a direct measure of the extent and distribution of green space coverage within the city's landscape.

(2) PD

$$\text{PD} = \left(\frac{n}{A_{\text{total}}} \right).$$

This metric measures the number of patches relative to the total area of the landscape. This metric primarily reflects the density of all patches of green space, without delving into the size or shape of each patch.

(3) LPI

$$\text{LPI} = \frac{\max_i (A_i)}{\sum_{i=1}^n A_i}.$$

This metric measures the percentage of the total green space that is made up of the largest patch of green space. A higher LPI value indicates a greater dominance of the largest patch within the city landscape.

(4) LSI

$$\text{LSI} = \left(\frac{\sum_{i=1}^n P_i}{4\sqrt{A_{\text{total}}}} \right).$$

P_i is the perimeter of patch i , calculated by summing the perimeters of all patches of green space and then dividing by four times the square root of the total landscape area. The square root of the area gives the side length of a square with the same area as the landscape, and multiplying by 4 gives the perimeter of that square. Thus, LSI measures the complexity of patch shapes relative to a square baseline, with higher values indicating more irregular and complex shapes compared to the simplicity of a square.

(5) SPLIT

$$\text{SPLIT} = \left(\frac{A_{\text{total}}^2}{\sum_{i=1}^n A_i^2} \right) \times 100.$$

This metric measures the degree of fragmentation of green space by comparing the size of all patches with the total landscape area. A higher SPLIT value indicates a greater degree of fragmentation, with smaller and more numerous patches spread throughout the landscape.

To calculate these metrics, we first identified the green space spatial distribution using the urban boundary data for all cities, to obtain the distribution of green spaces within each city's administrative area. We then processed these data individually into Fragstats (version 4.2) to compute all the landscape pattern indices for each city. All the identification and conversion processes were primarily carried out

using the Geopandas package (version 1.0.1) on the Python platform (version 3.12).

Considering the differing value ranges of these metrics and drawing from relevant study¹⁷, we opted to categorize the continuous value of each metric into three groups. This categorization could enable us to group the values of each metric, thereby satisfying the need for a meaningful stratified comparison and analysis across cities. It also helps avoid potential collinearity issues that might arise from finer grouping, while ensuring sufficient sample sizes within each group to maintain the reliability of our estimates. Specifically, we ranked all landscape metrics from lowest to highest and divided them into three equal groups: low, medium and high. Then, we used the correlation matrix method to test for potential collinearity issues among the five metrics after categorization. In addition, we calculated VIF values to further assess multicollinearity among the landscape metrics.

Analytical framework

Our analysis was confined to the period from May to October, when extreme heat events predominantly occur⁵¹. Regarding the method for identifying heatwaves, referring to relevant studies^{40,52}, we adopted the most commonly used heatwave definition approach based on percentile thresholds and consecutive days to ensure that heatwaves identified across different cities were comparable. Following established research practices^{40,53}, we used commonly used intensity percentiles, including the 92.5th and 95th percentiles, combined with duration criteria of two consecutive days and three or more consecutive days, creating four heatwave definitions: 92.5th percentile for ≥ 2 days, 92.5th percentile for ≥ 3 days, 95th percentile for ≥ 2 days and 95th percentile for ≥ 3 days.

We adopted a two-stage analytic framework, as done in previous multicity studies of heatwaves^{51,54–57}. For the first stage, the RRs of daily mortality related to heatwave exposure were calculated by comparing the heatwave days with non-heatwave days for each city. In this step, we used same model specifications as other heatwave-related studies^{51,54–56}, the detailed main model setting can be found in Supplementary Information. For the second stage, by using random effects meta-analyses with restricted maximum likelihood estimation⁵⁸, we pooled the coefficients and covariance matrixes of the cross-basis function that quantified the city-specific associations between heatwave exposure and daily mortality. The overall risks were pooled using different climate types, age groups and landscape metric groups.

To identify effect modification for the heatwave–mortality association, specifically the different metrics of green space patterns, we compared the cumulative RRs across different strata of potential modifiers⁵⁹. Specifically, we calculated *P*values to assess the differences between risk estimates from each of the subgroups using the multivariate Wald test, with a *P*value < 0.05 considered statistically significant⁶⁰.

Furthermore, to explore potential variations across different climatic conditions and age demographics, we examined whether the effects of different landscape pattern metrics varied across subgroups based on Köppen climate classification⁶¹ (temperate, continental and arid) and age groups (5–64 years, 65 years or older).

To test the robustness of our analysis, we conducted several sensitivity analyses. First, we obtained 2015 green space data for each city from the Global Forest Change dataset (version 1.3)⁶², which, primarily derived from Landsat remote sensing imagery, provides forest distribution data and has been widely used in related studies on the health impacts of green space⁶³. We used these forest distribution data as a proxy for green space, following the same analytical procedures as our primary analysis. In addition, we tested alternative heatwave definitions using daily maximum temperature instead of daily mean temperature. We also examined the sensitivity of our results to key model parameters, including degrees of freedom for time variable and humidity, and tested the potential confounding effects of air pollution by controlling for daily PM_{2.5} concentrations. Furthermore, to address

potential spatial representativeness issues of meteorological stations across different cities, we collected ERA5-Land gridded data within each city's boundaries and combined it with WorldPop 1-km population data to generate population-weighted daily mean temperature time series for each city during the study period (detailed weighting calculation procedures are provided in Supplementary Information).

Reporting summary

Further information on research design is available in the Nature Portfolio Reporting Summary linked to this article.

Data availability

Daily mortality data were obtained from China's Death Surveillance Points System, managed by the Chinese Center for Disease Control and Prevention. Due to data privacy regulations, these data cannot be publicly shared but may be requested from the Chinese Center for Disease Control and Prevention. Green space data are publicly available via the Essential Urban Land Use Categories in China (EULUC-China) dataset at <https://fuselab.hku.hk/dataset/>. Meteorological data are available via the China Meteorological Administration at <https://data.cma.cn/>. ERA5-Land reanalysis data are available via the Copernicus Climate Data Store at <https://cds.climate.copernicus.eu/>. Population data are available via WorldPop at <https://www.worldpop.org/>. Figure 1 and Supplementary Figs. 1 and 3 were created using Python 3.10 with Matplotlib v3.7.1 and Cartopy v0.21.1. The vector data for China's provincial administrative boundaries (including the Nine-Dash Line) were obtained from Xu Xinliang, Multi-year Provincial Administrative Division Boundary Data in China, Resource and Environmental Science Data Registration and Publication System (<https://www.resdc.cn/DOI/doi.aspx?DOIID=122>). Global coastlines and ocean boundaries (for regions outside China) are open-sourced and were derived from Natural Earth (<https://www.naturalearthdata.com/>). All spatial data were projected using the Plate Carrée projection (EPSG: 4326). Source data are provided with this paper.

Code availability

The analysis code used for the main statistical analysis in this study is available via GitHub at [https://github.com/chenghe1130/green space-Patterns-and-Heatwave-related-Mortality.git](https://github.com/chenghe1130/green-space-Patterns-and-Heatwave-related-Mortality.git).

References

1. Sun, Y. et al. Rapid increase in the risk of extreme summer heat in Eastern China. *Nat. Clim. Change* **4**, 1082–1085 (2014).
2. Yadav, N., Rajendra, K., Awasthi, A., Singh, C. & Bhushan, B. Systematic exploration of heat wave impact on mortality and urban heat island: a review from 2000 to 2022. *Urban Clim.* **51**, 101622 (2023).
3. Manoli, G. et al. Magnitude of urban heat islands largely explained by climate and population. *Nature* **573**, 55–60 (2019).
4. Zhao, L. et al. Global multi-model projections of local urban climates. *Nat. Clim. Change* **11**, 152–157 (2021).
5. Huang, W. T. K. et al. Economic valuation of temperature-related mortality attributed to urban heat islands in European cities. *Nat. Commun.* **14**, 7438 (2023).
6. Cleland, S. E., Steinhardt, W., Neas, L. M., West, J. J. & Rappold, A. G. Urban heat island impacts on heat-related cardiovascular morbidity: a time series analysis of older adults in US metropolitan areas. *Environ. Int.* **178**, 108005 (2023).
7. Hsu, A., Sheriff, G., Chakraborty, T. & Manya, D. Disproportionate exposure to urban heat island intensity across major US cities. *Nat. Commun.* **12**, 2721 (2021).
8. Wong, N. H., Tan, C. L., Kolokotsa, D. D. & Takebayashi, H. Greenery as a mitigation and adaptation strategy to urban heat. *Nat. Rev. Earth Environ.* **2**, 166–181 (2021).

9. Zhou, W., Yu, W., Zhang, Z., Cao, W. & Wu, T. How can urban green spaces be planned to mitigate urban heat island effect under different climatic backgrounds? A threshold-based perspective. *Sci. Total Environ.* **890**, 164422 (2023).
10. Wang, H. & Tassinari, L. G. Effects of green space morphology on mortality at the neighbourhood level: a cross-sectional ecological study. *Lancet Planet. Health* **3**, e460–e468 (2019).
11. Labib, S., Lindley, S. & Huck, J. J. Estimating multiple green space exposure types and their associations with neighbourhood premature mortality: a socioecological study. *Sci. Total Environ.* **789**, 147919 (2021).
12. Gunawardena, K. R., Wells, M. J. & Kershaw, T. Utilising green and bluespace to mitigate urban heat island intensity. *Sci. Total Environ.* **584**, 1040–1055 (2017).
13. Brown, R. D., Vanos, J., Kenny, N. & Lenzholzer, S. Designing urban parks that ameliorate the effects of climate change. *Landsc. Urban Plan.* **138**, 118–131 (2015).
14. Kabisch, N. et al. Impact of summer heat on urban park visitation, perceived health and ecosystem service appreciation. *Urban For. Urban Green.* **60**, 127058 (2021).
15. Li, Y., Ren, C., Ho, J. Y.-e. & Shi, Y. Landscape metrics in assessing how the configuration of urban green spaces affects their cooling effect: a systematic review of empirical studies. *Landsc. Urban Plan.* **239**, 104842 (2023).
16. Aram, F., García, E. H., Solgi, E. & Mansournia, S. Urban green space cooling effect in cities. *Heliyon* **5**, e01339 (2019).
17. Choi, H. M. et al. Effect modification of greenness on the association between heat and mortality: a multi-city multi-country study. *eBioMedicine* **84**, 104251 (2022).
18. Wang, H. et al. Where and how to invest in green space for optimal health benefits: a systematic review of green space morphology and human health relationships. *Lancet Planet. Health* **8**, e574–e587 (2024).
19. Wang, H. & Tassinari, L. G. Association between green space morphology and prevalence of non-communicable diseases mediated by air pollution and physical activity. *Landsc. Urban Plan.* **242**, 104934 (2024).
20. Tsai, W.-L. et al. Relationships between characteristics of urban green land cover and mental health in US metropolitan areas. *Int. J. Environ. Res. Public Health* **15**, 340 (2018).
21. Tsai, W.-L., Leung, Y.-F., McHale, M. R., Floyd, M. F. & Reich, B. J. Relationships between urban green land cover and human health at different spatial resolutions. *Urban Ecosyst.* **22**, 315–324 (2019).
22. Shen, Y.-S. & Lung, S.-C. C. Can green structure reduce the mortality of cardiovascular diseases?. *Sci. Total Environ.* **566**, 1159–1167 (2016).
23. Tamosiunas, A. et al. Accessibility and use of urban green spaces, and cardiovascular health: findings from a Kaunas cohort study. *Environ. Health* **13**, 20 (2014).
24. Seo, S., Choi, S., Kim, K., Kim, S. M. & Park, S. M. Association between urban green space and the risk of cardiovascular disease: a longitudinal study in seven Korean metropolitan areas. *Environ. Int.* **125**, 51–57 (2019).
25. Villeneuve, P. J. et al. A cohort study relating urban green space with mortality in Ontario, Canada. *Environ. Res.* **115**, 51–58 (2012).
26. Sinha, P. et al. Variation in estimates of heat-related mortality reduction due to tree cover in US cities. *J. Environ. Manag.* **301**, 113751 (2022).
27. Burkart, K. et al. Modification of heat-related mortality in an elderly urban population by vegetation (urban green) and proximity to water (urban blue): evidence from Lisbon, Portugal. *Environ. Health Perspect.* **124**, 927–934 (2016).
28. Masoudi, M. & Tan, P. Y. Multi-year comparison of the effects of spatial pattern of urban green spaces on urban land surface temperature. *Landsc. Urban Plan.* **184**, 44–58 (2019).
29. Imran, H. M., Kala, J., Ng, A. & Muthukumaran, S. Effectiveness of green and cool roofs in mitigating urban heat island effects during a heatwave event in the city of Melbourne in southeast Australia. *J. Cleaner Prod.* **197**, 393–405 (2018).
30. Fan, P., Xu, L., Yue, W. & Chen, J. Accessibility of public urban green space in an urban periphery: the case of Shanghai. *Landsc. Urban Plan.* **165**, 177–192 (2017).
31. Ekkel, E. D. & de Vries, S. Nearby green space and human health: evaluating accessibility metrics. *Landsc. Urban Plan.* **157**, 214–220 (2017).
32. Klemm, W., Heusinkveld, B. G., Lenzholzer, S., Jacobs, M. H. & Van Hove, B. Psychological and physical impact of urban green spaces on outdoor thermal comfort during summertime in The Netherlands. *Build. Environ.* **83**, 120–128 (2015).
33. Roe, J. J. et al. Green space and stress: evidence from cortisol measures in deprived urban communities. *Int. J. Environ. Res. Public Health* **10**, 4086–4103 (2013).
34. He, C., Zhou, L., Yao, Y., Ma, W. & Kinney, P. L. Cooling effect of urban trees and its spatiotemporal characteristics: a comparative study. *Build. Environ.* **204**, 108103 (2021).
35. Zhou, W., Wang, J. & Cadenasso, M. L. Effects of the spatial configuration of trees on urban heat mitigation: a comparative study. *Remote Sens. Environ.* **195**, 1–12 (2017).
36. Wang, C., Wang, Z.-H., Wang, C. & Myint, S. W. Environmental cooling provided by urban trees under extreme heat and cold waves in US cities. *Remote Sens. Environ.* **227**, 28–43 (2019).
37. Lüthi, S. et al. Rapid increase in the risk of heat-related mortality. *Nat. Commun.* **14**, 4894 (2023).
38. Yin, P. et al. Projection of mortality burden attributable to nonoptimum temperature with high spatial resolution in China. *Environ. Sci. Technol.* **58**, 6226–6235 (2024).
39. Liu, S. et al. An integrated national mortality surveillance system for death registration and mortality surveillance. *China. Bull. World Health Org.* **94**, 46–57 (2016).
40. Chen, R. et al. Association between ambient temperature and mortality risk and burden: time series study in 272 main Chinese cities. *BMJ* **363**, k4306 (2018).
41. Chen, R. et al. Fine particulate air pollution and daily mortality. A nationwide analysis in 272 Chinese cities. *Am. J. Resp. Crit. Care Med.* **196**, 73–81 (2017).
42. Yin, P. et al. Ambient ozone pollution and daily mortality: a nationwide study in 272 Chinese cities. *Environ. Health Perspect.* **125**, 117006 (2017).
43. Liu, C. et al. Ambient carbon monoxide and cardiovascular mortality: a nationwide time-series analysis in 272 cities in China. *Lancet Planet. Health* **2**, e12–e18 (2018).
44. Burkart, K. G. et al. Estimating the cause-specific relative risks of non-optimal temperature on daily mortality: a two-part modelling approach applied to the Global Burden of Disease Study. *Lancet* **398**, 685–697 (2021).
45. Gong, P. et al. Mapping essential urban land use categories in China (EULUC-China): preliminary results for 2018. *Sci. Bull.* **65**, 182–187 (2020).
46. Ke, Y., Xia, L., Wang, R., Liang, S. & Yang, Z. Construction of a methodology framework to characterize dynamic full-sector land-use carbon emissions embodied in trade. *Sci. Total Environ.* **913**, 169768 (2024).
47. Yan, X., Huang, Z., Ren, S., Yin, G. & Qi, J. Monthly electricity consumption data at 1 km × 1 km grid for 280 cities in China from 2012 to 2019. *Sci. Data* **11**, 877 (2024).
48. Kuang, W., Zhang, S., Li, X. & Lu, D. A 30 m resolution dataset of China's urban impervious surface area and green space, 2000–2018. *Earth Syst. Sci. Data* **13**, 63–82 (2021).

49. Tan, B., Wu, S., Su, S. & Weng, M. Spatial association of urban public green space supply and resident's health. *Urban Archit.* **24**, 57–61 (2018).
50. Wang, L., Jiang, X., Sun, W., Zhao, X. & Tang, J. Impact of urban built environment on respiratory health and its planning strategy: a case study of a district in Shanghai. *City Plan. Rev.* **42**, 15–22 (2018).
51. Yin, P. et al. The added effects of heatwaves on cause-specific mortality: a nationwide analysis in 272 Chinese cities. *Environ. Int.* **121**, 898–905 (2018).
52. Hundessa, S. et al. Global excess deaths associated with heatwaves in 2023 and the contribution of human-induced climate change. *Innovation* **6**, 101110 (2025).
53. Guo, Y. et al. Heat wave and mortality: a multicountry, multi-community study. *Environ. Health Perspect.* **125**, 087006 (2017).
54. Guo, Y. et al. Quantifying excess deaths related to heatwaves under climate change scenarios: a multicountry time series modelling study. *PLoS Med.* **15**, e1002629 (2018).
55. Kim, Y.-o., Lee, W., Kim, H. & Cho, Y. Social isolation and vulnerability to heatwave-related mortality in the urban elderly population: a time-series multi-community study in Korea. *Environ. Int.* **142**, 105868 (2020).
56. Zhao, Q. et al. Global, regional, and national burden of heatwave-related mortality from 1990 to 2019: a three-stage modelling study. *PLoS Med.* **21**, e1004364 (2024).
57. Gasparrini, A. & Armstrong, B. The impact of heat waves on mortality. *Epidemiology* **22**, 68–73 (2011).
58. Gasparrini, A. & Armstrong, B. Reducing and meta-analysing estimates from distributed lag non-linear models. *BMC Med. Res. Methodol.* **13**, 1 (2013).
59. Yang, Z. et al. Mortality risks associated with floods in 761 communities worldwide: time series study. *BMJ* **383**, e075081 (2023).
60. Chen, R. et al. Association of particulate air pollution with daily mortality: the China Air Pollution and Health Effects Study. *Am. J. Epidemiol.* **175**, 1173–1181 (2012).
61. Beck, H. E. et al. Present and future Köppen-Geiger climate classification maps at 1-km resolution. *Sci. Data* **5**, 180214 (2018).
62. Hansen, M. C. et al. High-resolution global maps of 21st-century forest cover change. *Science* **342**, 850–853 (2013).
63. Wu, L. & Chen, C. Does pattern matter? Exploring the pathways and effects of urban green space on promoting life satisfaction through reducing air pollution. *Urban For. Urban Green.* **82**, 127890 (2023).

Acknowledgements

This work was supported by National Natural Science Foundation of China (grant no. 82430105) and Shanghai Municipal Science and Technology Major Project (grant no. 2023SHZDXZ02).

Author contributions

C.H.: conceptualization, methodology, formal analysis, visualization, writing—original draft. P.Y.: data curation (mortality data), writing—review and editing. R.C.: supervision, funding acquisition, writing—review and editing. L.W.: data curation, validation, formal analysis. Y.W.: data curation, writing—review and editing. A.S.: methodology, writing—review and editing. H.K.: supervision, funding acquisition, project administration, writing—review and editing. M.Z.: supervision, resources, data curation (mortality data), writing—review and editing. All authors contributed to the interpretation of results and approved the final paper.

Competing interests

The authors declare no competing interests.

Additional information

Extended data is available for this paper at <https://doi.org/10.1038/s44360-025-00036-3>.

Supplementary information The online version contains supplementary material available at <https://doi.org/10.1038/s44360-025-00036-3>.

Correspondence and requests for materials should be addressed to Haidong Kan or Maigeng Zhou.

Peer review information *Nature Health* thanks Jun Yang and the other, anonymous, reviewer(s) for their contribution to the peer review of this work. Primary Handling Editor: Ben Johnson, in collaboration with the *Nature Health* team.

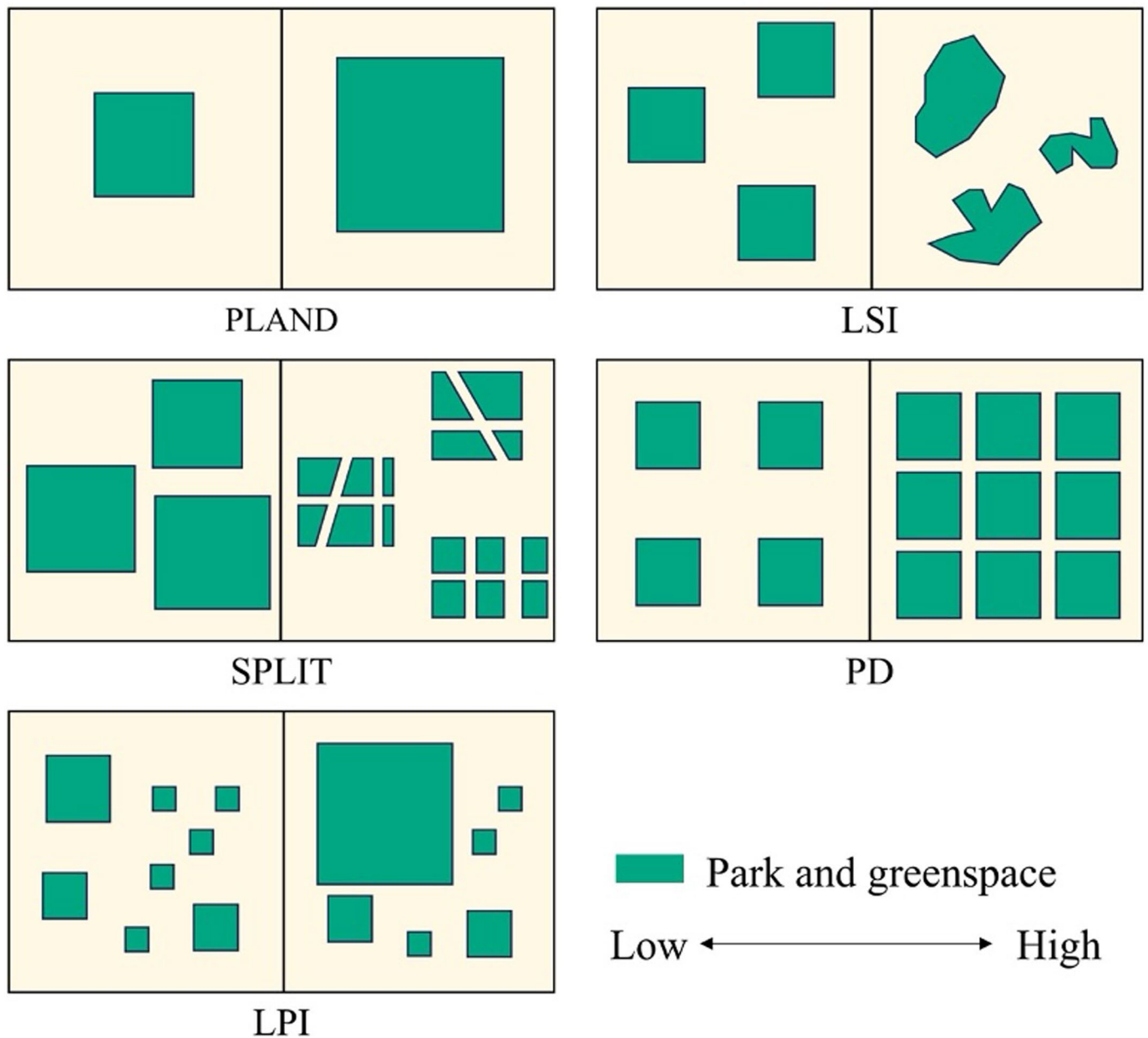
Reprints and permissions information is available at www.nature.com/reprints.

Publisher's note Springer Nature remains neutral with regard to jurisdictional claims in published maps and institutional affiliations.

Springer Nature or its licensor (e.g. a society or other partner) holds exclusive rights to this article under a publishing agreement with the author(s) or other rightsholder(s); author self-archiving of the accepted manuscript version of this article is solely governed by the terms of such publishing agreement and applicable law.

© The Author(s), under exclusive licence to Springer Nature Limited 2026

¹School of Public Health, Shanghai Institute of Infectious Disease and Biosecurity, Key Lab of Public Health Safety of the Ministry of Education and NHC Key Lab of Health Technology Assessment, Fudan University, Shanghai, China. ²Institute of Epidemiology, Helmholtz Zentrum München – German Research Center for Environmental Health, Neuherberg, Germany. ³National Center for Chronic and Noncommunicable Disease Control and Prevention, Chinese Center for Disease Control and Prevention, Beijing, China. ⁴Department of Environmental Science and Engineering, Fudan University, Shanghai, China. ⁵School of Geography and Tourism, Anhui Normal University, Wuhu, China. ⁶Children's Hospital of Fudan University, National Center for Children's Health, Shanghai, China. ⁷These authors contributed equally: Cheng He, Peng Yin, Renjie Chen.  e-mail: kanh@fudan.edu.cn; zhoumaigeng@ncncc.chinacdc.cn



Extended Data Fig. 1 | Conceptual diagram showing spatial patterns corresponding to different values of green space landscape metrics.
 Conceptual diagram illustrating spatial patterns represented by five green space landscape metrics. PLAND (Percentage of Landscape) measures total green space coverage. PD (Patch Density) indicates patch quantity per unit area. LPI (Largest

Patch Index) represents the dominance of the largest patch. LSI (Landscape Shape Index) quantifies boundary complexity, with higher values indicating more irregular shapes. SPLIT (Splitting Index) measures spatial fragmentation, with higher values indicating more dispersed patches.

Reporting Summary

Nature Portfolio wishes to improve the reproducibility of the work that we publish. This form provides structure for consistency and transparency in reporting. For further information on Nature Portfolio policies, see our [Editorial Policies](#) and the [Editorial Policy Checklist](#).

Statistics

For all statistical analyses, confirm that the following items are present in the figure legend, table legend, main text, or Methods section.

n/a Confirmed

- The exact sample size (n) for each experimental group/condition, given as a discrete number and unit of measurement
- A statement on whether measurements were taken from distinct samples or whether the same sample was measured repeatedly
- The statistical test(s) used AND whether they are one- or two-sided
Only common tests should be described solely by name; describe more complex techniques in the Methods section.
- A description of all covariates tested
- A description of any assumptions or corrections, such as tests of normality and adjustment for multiple comparisons
- A full description of the statistical parameters including central tendency (e.g. means) or other basic estimates (e.g. regression coefficient) AND variation (e.g. standard deviation) or associated estimates of uncertainty (e.g. confidence intervals)
- For null hypothesis testing, the test statistic (e.g. F , t , r) with confidence intervals, effect sizes, degrees of freedom and P value noted
Give P values as exact values whenever suitable.
- For Bayesian analysis, information on the choice of priors and Markov chain Monte Carlo settings
- For hierarchical and complex designs, identification of the appropriate level for tests and full reporting of outcomes
- Estimates of effect sizes (e.g. Cohen's d , Pearson's r), indicating how they were calculated

Our web collection on [statistics for biologists](#) contains articles on many of the points above.

Software and code

Policy information about [availability of computer code](#)

Data collection

Geospatial data processing was conducted using Python version 3.12 with the Geopandas package version 1.0.1 to extract and process greenspace distribution from the EULUC-China dataset within city boundaries. Landscape pattern metrics were calculated using Fragstats version 4.2. Meteorological data were directly obtained from the China Meteorological Administration's monitoring stations without requiring custom software. For sensitivity analyses, we downloaded ERA5-Land reanalysis data from the Copernicus Climate Data Store and WorldPop gridded population data for population-weighted temperature calculations. Mortality data were obtained directly from China's Death Surveillance Points System without additional software processing.

Data analysis

Statistical analyses were conducted in R version 4.4.2 using the dlnm package version 2.4.7 for distributed lag non-linear models and mvmeta package version 1.0.3 for meta-analysis. The analysis code is available at: <https://github.com/chenghe1130/Greenspace-Patterns-and-Heatwave-related-Mortality.git>.

For manuscripts utilizing custom algorithms or software that are central to the research but not yet described in published literature, software must be made available to editors and reviewers. We strongly encourage code deposition in a community repository (e.g. GitHub). See the Nature Portfolio [guidelines for submitting code & software](#) for further information.

Data

Policy information about [availability of data](#)

All manuscripts must include a [data availability statement](#). This statement should provide the following information, where applicable:

- Accession codes, unique identifiers, or web links for publicly available datasets
- A description of any restrictions on data availability
- For clinical datasets or third party data, please ensure that the statement adheres to our [policy](#)

Daily mortality data were obtained from China's Death Surveillance Points System, managed by the Chinese Center for Disease Control and Prevention. Due to data privacy regulations, these data cannot be publicly shared but may be requested from the Chinese Center for Disease Control and Prevention. Green space data are publicly available from the Essential Urban Land Use Categories in China (EULUC-China) dataset at <https://fuselab.hku.hk/dataset/>. Meteorological data are available from the China Meteorological Administration at <https://data.cma.cn/>. ERA5-Land reanalysis data are available from the Copernicus Climate Data Store at <https://cds.climate.copernicus.eu/>. Population data are available from WorldPop at <https://www.worldpop.org/>.

Research involving human participants, their data, or biological material

Policy information about studies with [human participants or human data](#). See also policy information about [sex, gender \(identity/presentation\), and sexual orientation](#) and [race, ethnicity and racism](#).

Reporting on sex and gender

This study used aggregated mortality data from national death surveillance system without individual-level information on sex or gender. All analyses were conducted at the city level using total non-accidental mortality counts. Sex- and gender-disaggregated analyses were not performed as the study focused on overall population-level heatwave-related mortality risks and their modification by greenspace landscape patterns.

Reporting on race, ethnicity, or other socially relevant groupings

No race, ethnicity, or other socially constructed groupings were used in this study.

Population characteristics

The study population comprised all residents in 265 Chinese cities during 2013–2019, with an average city population of 3,413,322 (range: 509,639 to 29,454,867). Mortality analyses were stratified by age groups: 5–64 years and ≥ 65 years.

Recruitment

Not applicable.

Ethics oversight

This study only involved secondary analysis, no ethics approval was required.

Note that full information on the approval of the study protocol must also be provided in the manuscript.

Field-specific reporting

Please select the one below that is the best fit for your research. If you are not sure, read the appropriate sections before making your selection.

Life sciences Behavioural & social sciences Ecological, evolutionary & environmental sciences

For a reference copy of the document with all sections, see nature.com/documents/nr-reporting-summary-flat.pdf

Behavioural & social sciences study design

All studies must disclose on these points even when the disclosure is negative.

Study description

This is a quantitative ecological time-series study examining the association between greenspace landscape patterns and heatwave-related mortality across 265 Chinese cities from 2013 to 2019.

Research sample

The research sample consisted of 265 prefecture-level or above cities in mainland China with mortality data from China's Death Surveillance Points System. The sample included cities with an average daily mortality count of at least 3 deaths and a total population of at least 200,000. Cities were distributed across 31 provincial administrative regions, representing over 80% of all prefecture-level and above cities in China.

Sampling strategy

Cities were selected using predefined inclusion criteria to ensure adequate statistical power for time-series analysis. We excluded cities with fewer than three average daily deaths, total population below 200,000, and insufficient green space coverage (total area $<0.01\%$). This stratified approach ensured sufficient sample sizes for reliable estimates while maintaining geographic representativeness.

Data collection

Daily mortality data were obtained from China's Death Surveillance Points System, a well-established national death registry covering all prefecture-level and above cities. Meteorological data (daily mean temperature and relative humidity) were collected from fixed monitoring stations operated by the China Meteorological Administration. Greenspace distribution data were extracted from the EULUC-China dataset, a parcel-level land use classification dataset developed using 10-meter resolution satellite imagery, OpenStreetMap, and location-based service data.

Timing

Data collection period: 2013 to 2019 for mortality and meteorological data.

Data exclusions

Seven cities were excluded due to insufficient green space areas (total coverage <0.01%). Cities with fewer than three average daily deaths or total population below 200,000 were also excluded to ensure adequate statistical power.

Non-participation

Not applicable. This study used complete surveillance data from existing national systems without individual-level participation or recruitment.

Randomization

Not applicable. This was an observational ecological study without experimental intervention or random allocation.

Reporting for specific materials, systems and methods

We require information from authors about some types of materials, experimental systems and methods used in many studies. Here, indicate whether each material, system or method listed is relevant to your study. If you are not sure if a list item applies to your research, read the appropriate section before selecting a response.

Materials & experimental systems

n/a	Involved in the study
<input checked="" type="checkbox"/>	Antibodies
<input checked="" type="checkbox"/>	Eukaryotic cell lines
<input checked="" type="checkbox"/>	Palaeontology and archaeology
<input checked="" type="checkbox"/>	Animals and other organisms
<input checked="" type="checkbox"/>	Clinical data
<input checked="" type="checkbox"/>	Dual use research of concern
<input checked="" type="checkbox"/>	Plants

Methods

n/a	Involved in the study
<input checked="" type="checkbox"/>	ChIP-seq
<input checked="" type="checkbox"/>	Flow cytometry
<input checked="" type="checkbox"/>	MRI-based neuroimaging

Plants

Seed stocks

Not applicable.

Novel plant genotypes

Not applicable.

Authentication

Not applicable.